Surface Technology White Papers
98 (8), 16-25 (November 2011)

Electrodeposition and Characterization of Nickel–Titania Nanocomposite Coatings from Gluconate Baths

by
M.S. Ali Eltoum,[1] A.M. Baraka,[2] M.S. Morsi[2] and Elfatih A. Hassan[1]*
[1]Scientific Laboratories Department, Faculty of Science, Sudan University of Science & Technology, Khartoum, Sudan
[2]Chemistry Department, Faculty of Science, Cairo University, Cairo, Egypt

ABSTRACT

Ni-TiO_2 nanocomposites with varying titania content were electrodeposited on copper substrates employing a gluconate electrolyte. The changes in microstructure and corrosion behavior of electrodeposited nickel with respect to titania addition were studied. The titania content in the coatings increased with increasing titania content in the bath and decreased at high current density. The effect of pH shows an increase in titania up to pH 8. Enhancement of hardness and corrosion resistance was observed via incorporation of titania in the nickel matrix. The addition of TiO_2 nanoparticles to the bath affects the microstructure and morphology of the nickel matrix, as indicated by x-ray diffraction (XRD) and scanning electron microscopy (SEM).

Keywords: Ni-TiO_2 nanocomposite, electrodeposition, corrosion resistance, polarization curves

Introduction

Nanocomposites consisting of ultrafine particles of pure metals, ceramics and organic materials in an inert metal matrix have attracted extensive attention in science and technology for decades,[1-3] due to their beneficial electrical,[4,5] optical,[5-7] magnetic[8,9] and mechanical[10-13] properties. In order to improve the useful properties of nickel layers, the coatings have been co-deposited from baths containing metal oxides (TiO_2, Al_2O_3, Sc_2O_3, and NiO), carbide, nitrides or PTFE.[14-17] Such a procedure has led to the production of layers with a composite structure, and characterized by special properties, such as good catalytic activity, good corrosion resistance, increased hardness and resistance to high temperatures. Methods available for the preparation of nanocrystalline films include candidates based on chemical solution growth, sol-gel chemistry and slurry spray/brush-coat techniques[18] and occlusion electrodeposition.[7] Research related to Ni-TiO_2 composite coatings has demonstrated that the codeposition percentage of nano-titania particles is difficult to control quantitatively, because the particles are frequently agglomerated in the metal-matrix, as well as in the electrolyte, due to their significant high surface energy. Given that, TiO_2 particles seem to incorporate only to a limited extent, when compared to other ceramic particles, such as SiC particles.[19]

A survey of the literature shows that gluconate electrolytes have been used to electroplate metals such as nickel,[20] copper,[21] tin[22] and zinc.[23] Organic additives have been found to affect the electrothrowing power of nickel from sulfate, chloride and Watts baths. The objective of the present study is to electrodeposit a nickel-titania composite from a gluconate bath in order to determine the dependence of coating characteristics on several electroplating variables and to characterize the coatings by SEM, EDX and XRD and examining their hardness and corrosion resistance.

Experimental

The plating bath used (described in Table 1) was freshly prepared from reagent grade chemicals and doubly distilled water. Copper sheet cathodes and pure nickel sheet anodes, both of dimensions 2×2 cm^2 were used. The copper sheet cathodes were mechanically polished with different grade emery papers and then immersed in a pickling solution (300 mL H_2SO_4 + 100 mL HNO_3 + 5 mL HCl + 595 mL doubly-distilled water) for 1 min, washed with distilled water, rinsed with acetone, dried and finally weighed. The pH was measured using Microprocessor pH/mV/°C Meter (Model CP 5943-45USA) and adjusted with a 20%

---

[*] Corresponding author:
M.S. Ali Eltoum
Scientific Laboratories Department
Faculty of Science
Sudan University of Science & Technology
Khartoum, Sudan
Phone.: +20 166850404; +249912694177.
E-mail: tetez74@yahoo.com

NaOH solution. The temperature was controlled by using hot plate-magnetic stirrer (Philip Harris Ltd). Direct current was supplied by a DC power supply unit (GP-4303D). The copper cathodes were weighed before and after electrodeposition for a certain period of time and at fixed current density. From the change in weights of the cathodes, the deposited weight was calculated. The composition was determined using the following procedure:

1. The coating layer was stripped using 10% H_2SO_4 solution. The next step was to use it as an anode in an electroplating cell by which the coating layer was dissolved in the solution, which was then diluted to 250 mL with doubly-distilled water.
2. Analysis was done using atomic absorption spectrophotometry (Perkin-Elmer 3100, Germany).
3. The solution obtained was further diluted by dissolving 5 mL in doubly-distilled water to 250 mL.
4. Nickel standard solutions for the elements to be detected were prepared (1 g Ni metal in (1+1) HNO_3, diluted to 1 L with 1 vol% HNO_3), Ni, air-acetylene flame gases, wavelength of 232 nm.
5. The titania weight was calculated by subtracting the obtained nickel weight from the total deposit weight.

The results were confirmed for some samples with EDX analysis.

The surface of the as-deposited nickel and nickel-titania was morphologically inspected using scanning electron microscopy (SEM; JEOL-5410 attached to an EDX unit). The phases of the surface and phase changes of the different coated substrates were investigated by using an x-ray diffractometer (Broker AXS-D8 X-ray diffractometer, Advance, Germany), with a copper target (Cu_λ = 1.54060 Å) and a nickel filter. The coating thickness was measured by taking a cross-section of the coated layer using a coating thickness / Neophot2-optical microscope (Germany). The Vickers microhardness of the deposits was measured under a 50-g load on the specimen material by using a Shimdzu Hardness tester. The electrochemical experiments were performed using a Volta Lab 40 (Model PGZ301) with the aid of commercial software (Volta Master 4 version 7.08). A saturated calomel electrode (SCE) and a platinized platinum black were used as the reference and auxiliary electrodes, respectively, with the various plated samples used as the working electrode. The electrochemical cell was filled with a 3.5% NaCl electrolyte. Volta Master 4 calculates and displays the corrosion rate, R_{corr}, in μm/year. This rate is calculated from the measured corrosion current density, i_{corr}, the density D, the atomic mass M and the valence V entered in the Tafel dialogue box. The calculation is performed as follows:

$$\text{Corrosion rate } (\mu\text{m/yr}) = [i_{corr}\ (\text{A/cm}^2) \times M\ (\text{g})] / [D\ (\text{g/cm}^3) \times V] \times 3270$$

With: 3270 = 0.01 × [1 yr (in sec) / 96497.8]; 1 Faraday = 96497.8 Coulombs.

Table 1 - The bath composition and operating conditions of nickel-titania composite process.

Nickel sulfate	0.2 mol/L
Boric acid	0.4 mol/L
Ammonium sulfate	0.4 mol/L
Sodium gluconate	0.2 mol/L
Titania (50 nm)	3 - 7 g/L
Temperature	30 - 70°C
Current density	2.5 - 7.5 A/dm^2
pH	6 - 10
Time	10 - 60 min
Stirring speed	150 rpm

The same bath composition was used for nickel electrodeposition without titania for comparison.

Results and discussion

Optimization of nickel-titania electrodeposition parameters:

The effect of current density on the coating thickness is illustrated in Fig. 1. It is clear from these results that the thickness increased with increasing current density up to 6.25 A/dm^2 and beyond that decreased gradually. This may be attributed to the fact that an increase in current density results in more rapid deposition of metal matrix and fewer particles are embedded in the coating. Hence, the metal deposition dominates the co-deposition process.[24]

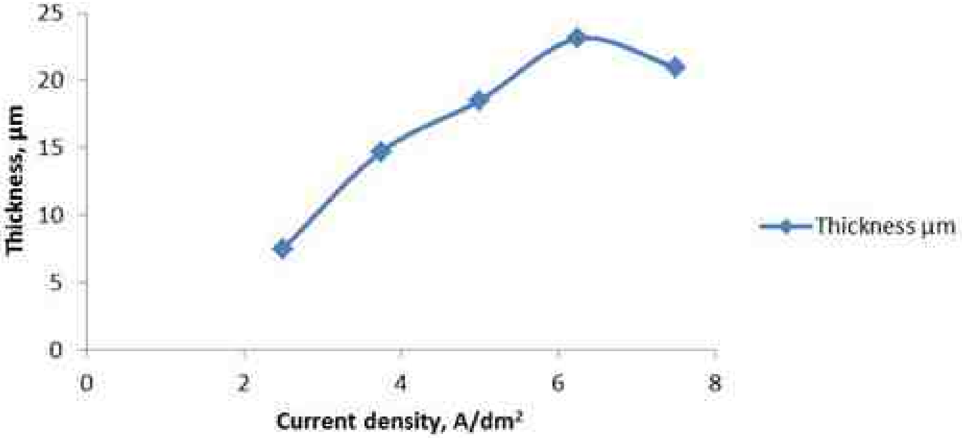

Figure 1 - Effect of current on the thickness of the composites from a bath containing 0.2 mol/L $NiSO_4$•$6H_2O$, 0.2 mol/L $C_6H_{11}NaO_7$, 6.0 g/L TiO_2, 0.4 mol/L boric acid, 0.4 mol/L $(NH_4)_2SO_4$, pH 8, Temperature 25°C, Time 20 min.

From Fig. 2, it is seen that the thickness of the composite is increased with increasing pH up to pH 8, after which the coating thickness is decreased due to the nickel hydroxide precipitation.

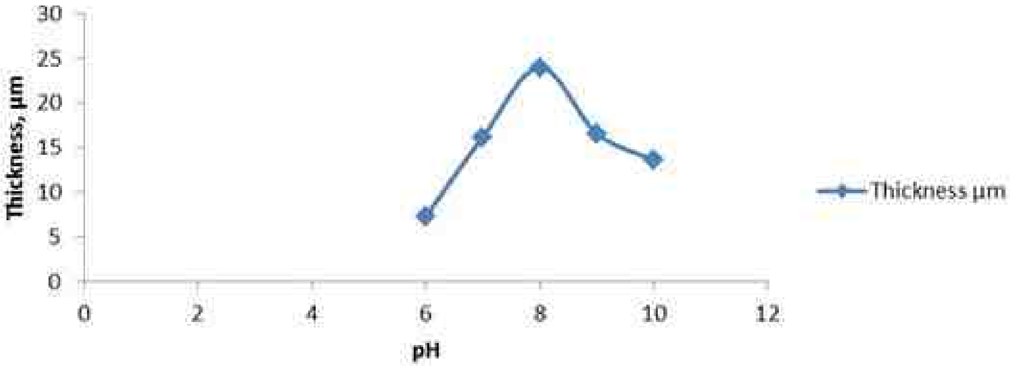

Figure 2 - Effect of pH on the thickness of the composites from a bath containing 0.2 mol/L $NiSO_4$•$6H_2O$, 0.2 mol/L $C_6H_{11}NaO_7$, 6.0 g/L TiO_2, 0.4 mol/L boric acid, 0.4 mol/L $(NH_4)_2SO_4$, Current density 6.2 A/dm^2, Temperature 25°C, Time 20 min.

The effect of plating time on the coating thickness is shown in Fig. 3. These results indicate that the thickness of coating increased with increasing plating time in accordance with Faraday's law.

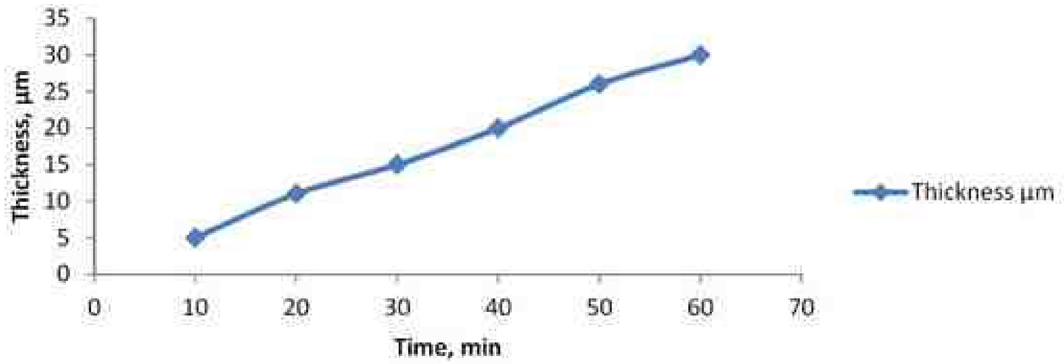

Figure 3 - Effect of process time on the thickness of the composites from a bath containing 0.2 mol/L $NiSO_4{\bullet}6H_2O$, 0.2 mol/L $C_6H_{11}NaO_7$, 6.0 g/L TiO_2, 0.4 mol/L boric acid, 0.4 mol/L $(NH_4)_2SO_4$, Current density 6.2 A/dm^2, Temperature 25°C, pH 8.

One of the important parameter in electroplating is the bath temperature. Figure 4 shows that the coating thickness is increased with increasing temperature up to 60°C. Beyond that point, hydrogen evolution hinders the composite deposition.

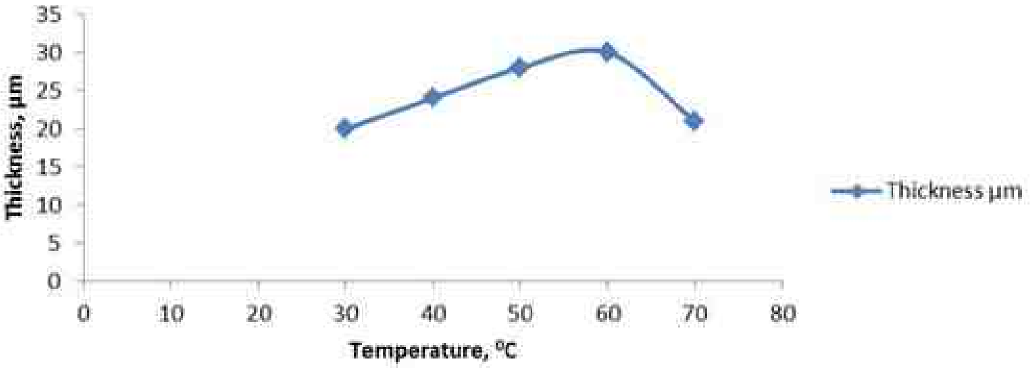

Figure 4 - Effect of temperature on the thickness of the composites from a bath containing 0.2 mol/L $NiSO_4{\bullet}6H_2O$, 0.2 mol/L $C_6H_{11}NaO_7$, 6.0 g/L TiO_2, 0.4 mol/L boric acid, 0.4 mol/L $(NH_4)_2SO_4$, Current density 6.2 A/dm^2, Time 20 min, pH 8.

Characterization of nickel-titania composites

It is interesting to note that the rate of particle incorporation is higher at low current densities and levels off at higher current densities, as seen in Fig. 5. This dependence of particle incorporation on the current density is consistent with Guglielmi's model.[25] At low current densities, the codeposition process is controlled by particle adsorption and hence particle incorporation is dominant.

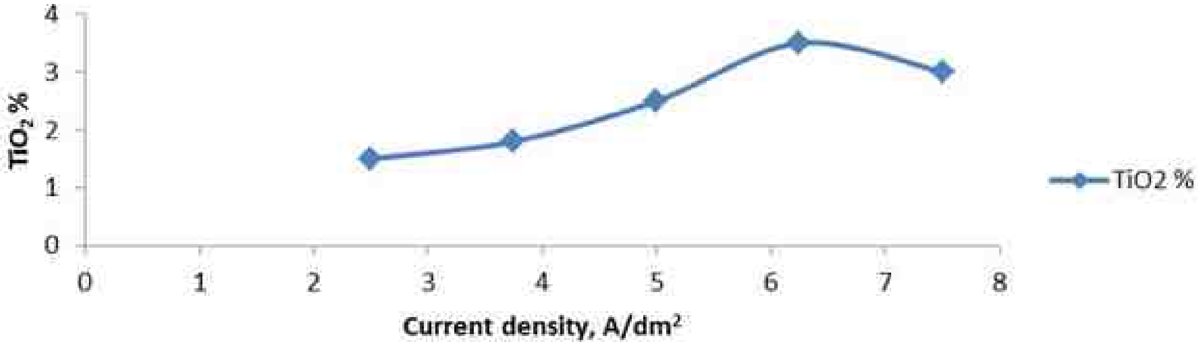

Figure 5 - Effect of current density on the TiO_2 content in the composites from a bath containing 0.2 mol/L $NiSO_4•6H_2O$, 0.2 mol/L $C_6H_{11}NaO_7$, 6.0 g/L TiO_2, 0.4 mol/L boric acid, 0.4 mol/L $(NH_4)_2SO_4$, pH 8, Temperature 25°C, Time 20 min.

Figures 6 and 7 show the EDX spectra of Ni-TiO_2 composites obtained at current densities of 6.25 and 3.75 A/dm^2, respectively.

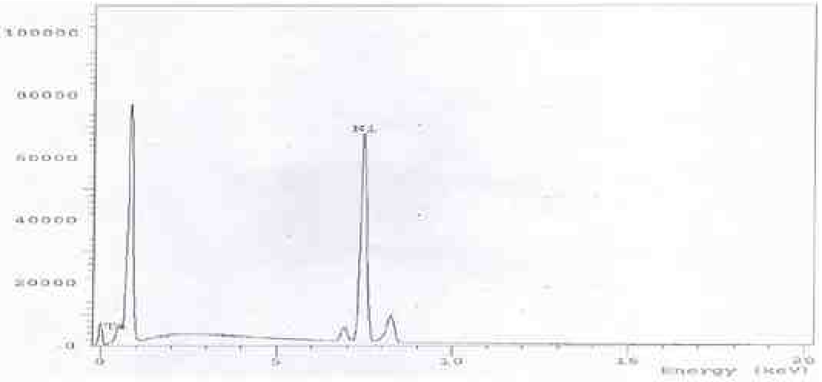

Figure 6 - EDX spectrum for 96.5 wt% Ni-3.5 wt% TiO_2 composite from a bath containing 0.2 mol/L $NiSO_4•6H_2O$, 0.2 mol/L $C_6H_{11}NaO_7$, 6.0 g/L TiO_2, 0.4 mol/L boric acid, 0.4 mol/L $(NH_4)_2SO_4$, pH 8, Temperature 25°C, Time 20 min, Current density 6.25 A/dm^2.

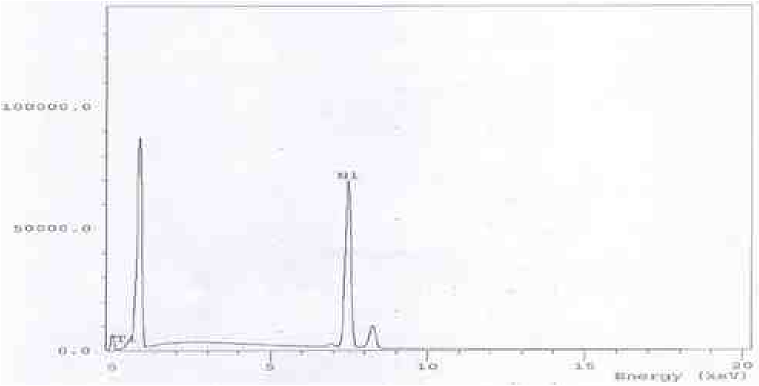

Figure 7 - EDX spectrum for 97.2 wt% Ni-1.8 wt% TiO_2 composites from a bath containing 0.2 mol/L $NiSO_4•6H_2O$, 0.2 mol/L $C_6H_{11}NaO_7$, 6.0 g/L TiO_2, 0.4 mol/L boric acid, 0.4 mol/L $(NH_4)_2SO_4$, pH 8, Temperature 25°C, Time 20 min, Current density 3.75 A/dm^2.

The x-ray diffraction spectra in Fig. 8 show that the codeposition of TiO_2 obviously affects the relative intensity corresponding to different crystal faces of nickel. The relative intensity corresponding to crystal face (111) decreases, but the relative intensity of crystal face (200) increases. For composite coatings, the peak of crystal face (220) is not clear. The peak of (311) becomes stronger with increasing TiO_2 content. Erler, *et al.*[26] demonstrated that the XRD patterns of nickel nanocomposite coatings indicate changes in texture of such coatings, which are dependent on the plating current density and the particle content in the electrolyte. The average grain size was 42 nm. This result is close to the results obtained by Sun and Li.[27]

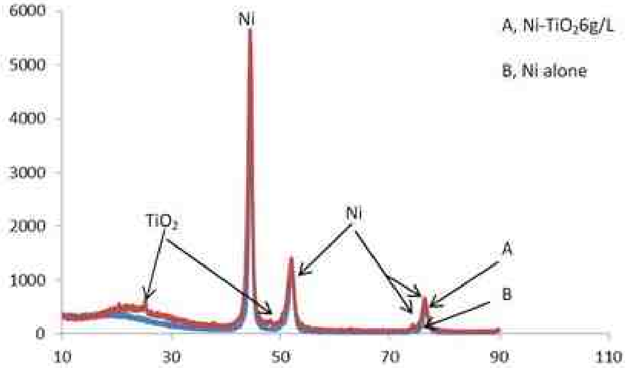

Figure 8 - XRD spectra for (a) 96.5 wt% Ni-3.5 wt% TiO_2 composite from a bath containing 0.2 mol/L $NiSO_4•6H_2O$, 0.2 mol/L $C_6H_{11}NaO_7$, 6.0 g/L TiO_2, 0.4 mol/L boric acid, 0.4 mol/L $(NH_4)_2SO_4$, pH 8, Temperature 25°C, Time 20 min, Current density 6.25 A/dm^2; (b) nickel obtained from a gluconate bath containing 0.2 mol/L $NiSO_4•6H_2O$, 0.2 mol/L $C_6H_{11}NaO_7$, 0.4 mol/L boric acid, 0.4 mol/L $(NH_4)_2SO_4$, pH 8, Temperature 25°C, Time 20 min, Current density 2.5 A/dm^2.

The effect of TiO_2 concentration in the plating bath on the titania content in the composite is shown in Fig. 9 and was confirmed by the previously discussed EDX spectrum of Fig. 6. There was an increase in the particle incorporation with increasing particle content of the electrolyte. This behavior can be understood in terms of the two-step adsorption model of Guglielmi,[25] which quantitatively describes the influence of particle content in the electrolyte and the current density on the particle incorporation. In the first step, the particles become loosely adsorbed on the electrode surface and stay in equilibrium with the particles in solution.[28] The particles are still surrounded by a thin layer of adsorbed ions and solvent molecules governing the interaction between the particles and the electrode. An increase of the particle concentration in the electrolyte causes an increase of the particle adsorption rate. In the second step, the shell of adsorbed ions is broken by the electrical field at the interface followed by a strong adsorption of the particles onto the electrode. This result is in agreement with results obtained by Thiemig and Bund.[29] The asymptotic behavior of the particle incorporation with increasing current density can be attributed to the faster deposition of the metal matrix.[30]

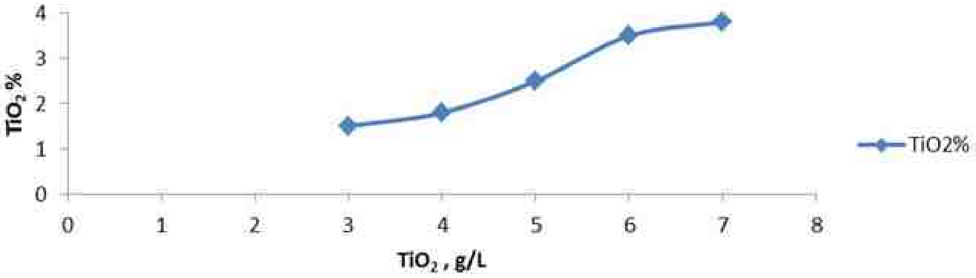

Figure 9 - Effect of TiO_2 content in the bath on the wt% TiO_2 in the deposit from a bath containing, 0.2 mol/L $NiSO_4•6H_2O$, 0.2 mol/L $C_6H_{11}NaO_7$, 0.4 mol/L boric acid, 0.4 mol/L $(NH_4)_2SO_4$, pH 8, Current density 6.25 A/dm^2, Temperature 25°C, Time 20 min.

The effect of pH on the titania content of the composite is shown in Fig. 10. The titania content increased with pH and decreased beyond pH 8 due to the formation of $Ni(OH)_2$. The nickel films from the alkaline bath contained significantly higher amounts of particles. There seems to be a tendency that negatively-charged oxide particles are preferentially codeposited in cathodic processes, at least in solutions containing divalent cations. In order to explain this counter-intuitive behavior, electrostatic model has been proposed[31-33] which takes into account the charge distribution on the particle and on the electrode surface. In the alkaline electrolyte, the TiO_2 nanoparticles are negatively charged, whereas in an acidic solution, they bear a positive charge. Under the conditions of the nickel electroplating process, the electrode bears excess negative charges.[33] According to the model, negatively-charged particles are preferentially attracted by the excess positive charges in the electrolytic part of the electrical double layer of the electrode. When the particle comes close to the electrode, the shell of adsorbed ions on the particle is stripped off within the electrical double layer. Finally the particle becomes incorporated into the growing metal layer.

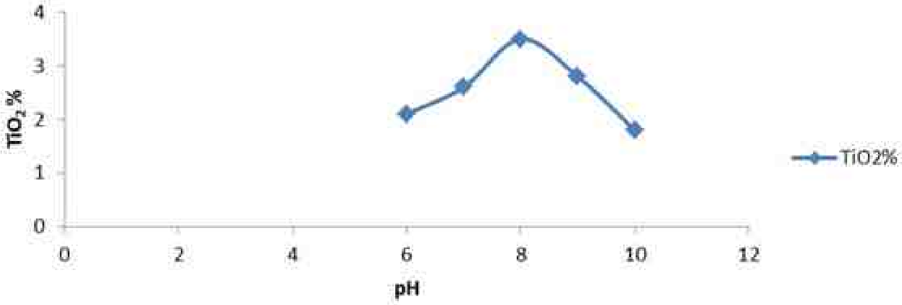

Figure 10 - Effect of pH on the wt% TiO_2 in the deposit on the composites from a bath containing 0.2 mol/L $NiSO_4•6H_2O$, 0.2 mol/L $C_6H_{11}NaO_7$, 6.0 g/L TiO_2, 0.4 mol/L boric acid, 0.4 mol/L $(NH_4)_2SO_4$, Current density 6.2 A/dm^2, Temperature 25°C, Time 20 min.

Surface morphology of the Ni-TiO_2 composite coating:

The addition of titania nanoparticles to the bath obviously affects the surface morphology of the coatings, as shown in Figs. 11 and 12. The titania particles appear as light spots in the darker nickel matrix. Because of the addition of TiO_2 nanoparticles to the bath, the microstructure of the nickel matrix changed from spherical (Fig. 11) to granular (Fig. 12).

Figure 11 - SEM of nickel deposited from a bath containing 0.2 mol/L $NiSO_4•6H_2O$, 0.2 mol/L $C_6H_{11}NaO_7$, 0.4 mol/L boric acid and 0.4 mol/L ammonium sulfate at pH 8, Time 20 min, Temperature 25°C and Current density 2.5 A/dm^2.

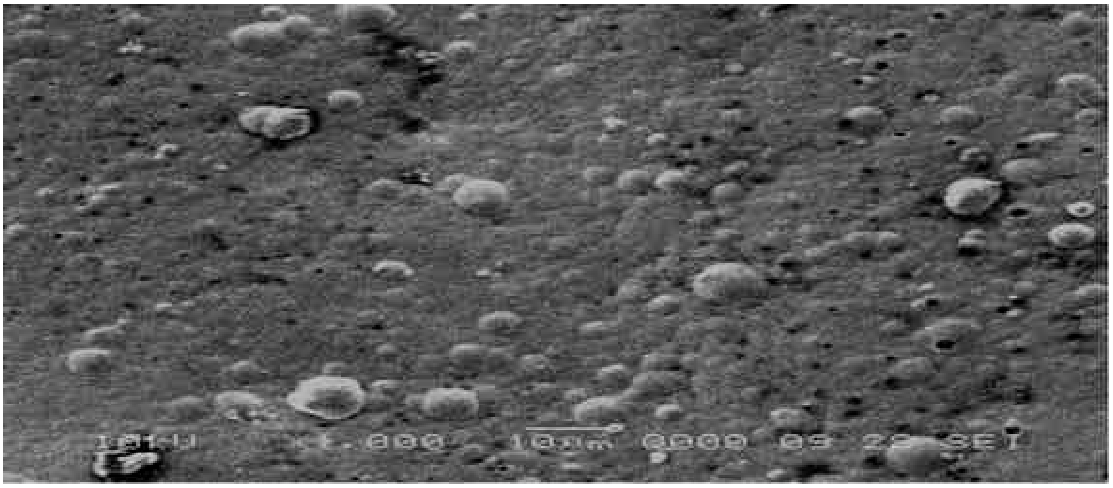

Figure 12 - SEM of a 96.5 wt% Ni-3.5 wt% TiO_2 composite coating from a bath containing 0.2 mol/L $NiSO_4$•$6H_2O$, 0.2 mol/L $C_6H_{11}NaO_7$, 0.4 mol/L boric acid, 0.4 mol/L $(NH_4)_2SO_4$, pH 8, Current density 6.25 A/dm^2, Temperature 25°C, Time 20 min.

Microhardness

The incorporation of TiO_2 in the coating increased the hardness. In the case of 3.5 wt% TiO_2, the observed hardness was 440HV50, instead of 340HV50 in the case of the pure nickel coating.

Potentiodynamic polarization curves

The corrosion behavior of Ni-TiO_2 composites, nickel deposited from gluconate and an unplated copper substrate for comparison is illustrated in Fig. 13 and Table 2. It can be seen from the curves that a passive region was observed for the composite, indicating that the anodic reaction was inhibited to a certain extent with the increase of anodic potential. In addition, much lower anodic current densities are observed, compared with the nickel deposit or the copper substrate, as confirmed by the lower corrosion rate observed.

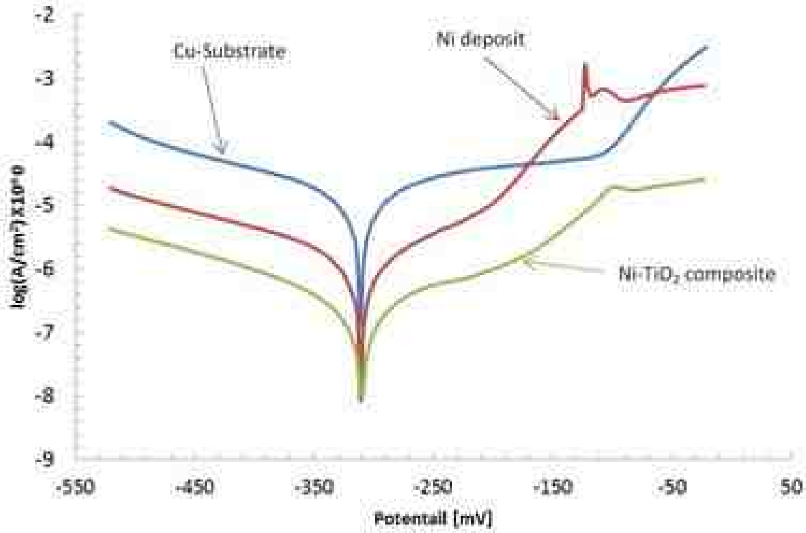

Figure 13 - Potentiodynamic polarization curves of for the copper substrate, nickel deposit and Ni-TiO_2 observed in 3.5% NaCl solution.

Table 2 - Corrosion data for the copper substrate, nickel deposit and Ni-TiO_2 obtained from immersion in 3.5% NaCl solution.

	E_{corr} (i=0), mV	i_{corr}, $\mu A/cm^2$	R_p, $k\Omega \cdot cm^2$	Beta *a*, mV	Beta *c*, mV	Corr. rate, µm/yr
Cu substrate	-315.0	6.2359	1.93	73.4	-82.7	72.40
Ni-gluconate	-228.7	0.5479	17.83	64.3	-66.2	6.362
Ni-TiO_2	-264.3	120.11	100.77	66.5	-78.8	1.394

Conclusion

In the electrodeposition of Ni-TiO_2 nanocomposites, the amount of TiO_2 incorporated is directly increased with an increasing amount of particles present in the bath. However, the applied current density and pH of the electrolytic solution critically affect the amount of incorporation. The amount of particles in the deposit increases with increasing current density and pH to certain degree and then decreased (beyond 6.25 A/dm^2 and pH 8 in this study, respectively). The incorporation of TiO_2 nanoparticles affects the structure of the nickel matrix and enhances the hardness and corrosion resistance, compared to the unplated copper substrate and nickel deposited without TiO_2.

References

1. J.P. Celis, J.R. Roos & C. Buelens, *J. Electrochem. Soc.*, **134** (6), 1402 (1987).
2. C.T.J. Low, R.G.A. Wills & F.C. Walsh, *Surf. Coat. Technol.*, **201** (1-2), 371 (2006).
3. J.L. Stojak, J. Fransaer & J.B. Talbot, "Chapter 4 - Review of Electrocodeposition," in: R.C. Alkire, D.M. Kolb (Eds.), *Advances in Electrochemical Science and Engineering - Volume 7*, Wiley-VCH Verlag, Weinheim, Germany, 2002.
4. V. Medelienė, V. Stankevič & G. Bikulčius, *Surf. Coat. Technol.*, **168** (2-3), 161 (2003).
5. N.R. de Tacconi, H.Wenren & K. Rajeshwar, *J. Electrochem. Soc.*, **144** (9), 3159 (1997).
6. N.R. de Tacconi, C.A. Boyles & K. Rajeshwar, *Langmuir*, **16** (13), 5665 (2000).
7. M. Zhou, N.R. de Tacconi & K. Rajeshwar, *J. Electroanal. Chem.*, **421** (1-2), 111 (1997).
8. D. Thiemig, *et al.*, *Thin Sold Films*, **517** (5), 1636 (2009).
9. A. Roldan, *et al.*, *J. Appl. Electrochem.*, **37** (5), 575 (2007).
10. A.F. Zimmerman, *et al.*, *Mater. Sci. Eng. A*, **328** (1-2), 137 (2002).
11. S. Veprek & A.S. Argon, *Surf. Coat. Technol.*, **146–147**, 175 (2001).
12. Y-J. Xue, D. Zhu & F. Zhao, *J. Mater. Sci.*, **39** (12), 4063 (2004).
13. S. Tao & D.Y. Li, *Nanotechnology*, **17** (1), 65 (2006).
14. C.W. Yuen & H.W. Kui, *J. Mater. Res. USA*, **13** (11), 3043 (1998).
15. D.S.W. Dos Santos & P.E.V. De Miranda, *Int. J. Hydrogen Energy*, **23** (11), 1011 (1998).
16. J. Niedbała, *et al.*, *Thin Solid Films*, **266** (2), 113 (1995).
17. B. Losiewicz, *et al.*, *Thin Solid Films*, **349** (1-2), 43 (1999).
18. M. Zhou, *et al.*, *J. Electroanal. Chem.*, **402** (1-2), 221 (1996).
19. S. Spanou, E.A. Pavlatou & N. Spyrellis, *Electrochimica Acta.*, **54** (9), 2547 (2009).
20. E.A. Abd El Meguid, S.S. Abd El Rehim & E. M. Moustafa, *Trans. IMF*, **77**, 188 (1999).
21. S.S. Abd El Rehim, S.M. Sayyah & M.M. El Deeb, *Appl. Surf. Sci.*, **165** (4), 249 (2000).
22. S.S. Abd El Rehim, S.M. Sayyah & M.M. El Deeb, *Plating & Surface Finishing,* **87** (9), 93 (2000).
23. S.M.Rashwan, *et al.*, *Mans. Sci. Bull. A (Chemistry)*, **27**, 121 (2000).
24. Q. Feng, *et al.*, *Appl. Surf. Sci.*, **254** (8), 2262 (2008).
25. J. Fransaer, J.P. Celis & J.R. Roos, *J. Electrochem. Soc.*, **139** (2), 413 (1992).
26. F. Erler, *et al.*, *Electrochim. Acta.*, **48** (20-22), 3063 (2003).
27. X.J. Sun & J.G. Li, *Tribol. Lett.*, **28** (3), 223 (2007).
28. B.J. Hwang & C.S. Hwang, *J. Electrochem. Soc.*, **140** (4), 979 (1993).
29. D. Thiemig & A. Bund, *Surf. Coat. Technol.*, **202** (13), 2976 (2008).
30. L. Shi, *et al.*, *Appl. Surf. Sci.*, **252** (10), 3591 (2006).
31. F. Wünsche, A. Bund & W. Plieth, *J. Solid State Electrochem.*, **8** (3), 209 (2004).
32. A. Bund & D. Thiemig, *J. Appl. Electrochem.*, **37** (3), 345 (2007).
33. A. Bund & D. Thiemig, *Surf. Coat. Technol.* **201** (16-17), 7092 (2007).

About the lead author

Dr. Mohammed Sulieman Ali Eltoum was born May 9, 1974 in Khartoum, Sudan. He holds a B.SC. degree in Laboratory Technology - Chemistry, as well as M.Sc and Ph.D degrees in Chemistry. His research interests include electro- and electroless plating of metals.